Available online at www.sciencedirect.com
SCIENCE DIRECT®
Cement and Concrete Research 36 (2006) 921 – 928
Cement and Concrete Research

Surface and internal deterioration of concrete due to saline and non-saline freeze–thaw loads

Vesa Penttala *

Building Materials Technology, Department of Civil and Environmental Engineering, Helsinki University of Technology, P.O. Box 2100, FIN-02015 HUT, Finland

Received 8 December 2004; accepted 9 October 2005

Abstract

Concrete deterioration due to frost action in non-saline and saline environments was studied statistically. The most significant variables affecting the freeze–thaw durability of concrete were calculated statistically and contours of estimated response surface were produced. Water–cement ratio and air content of the concretes were the most dominant variables affecting the internal and surface damage caused by the freezing and thawing loads. In the non-saline environment, water curing improved the R^2 values of the developed deterioration models in the surface scaling part of the tests. In the internal damage tests, the curing measures did not improve the statistical relevancy of the estimated response surfaces. In the saline freeze–thaw tests, high-strength concretes were studied. When water–binder ratio was below 0.42 internal deterioration was the governing freeze–thaw damage mechanism which needed larger air content compared to surface scaling.

Keywords: Concrete (E); Freezing and thawing (C); Modeling (E); Surface layer (B); Internal damage

1. Introduction

Almost one third of the concrete volume cast in the Nordic countries must possess adequate freeze–thaw durability. The majority of concrete durability research and test methods concentrate on the degradation of the concrete surface due to the freezing and thawing loads, while only during the last decade has the internal damage of the frost action gained increasing attention. It has been noticed that internal damage has been the dimensioning criterion in concretes produced with a low water–binder ratio.

The two classical freezing and thawing theories of concrete are based on the research work by Powers et al. [1–5]. The theory of hydraulic pressure is considered valid nowadays only in very saturated conditions and even Powers replaced it by the theory of osmotic pressure. In these theories, the direction of the pore water movements are inverted. In the theory of hydraulic pressure, the pore water is considered to move from those parts of the capillary space in which ice is first generated towards other parts of the concrete matrix. However, test results and also theoretical considerations have shown that the direction of water movement during freezing is in the opposite direction. The unfrozen pore water in the nearby smaller pore spaces is drawn to those parts of the pore system in which ice is first formed. In the theory of osmotic pressure, Powers deduced that the pore water is moving in this direction due to the osmotic pressure caused by the dissolved substances (mainly Ca^{2+}, K^+, and Na^+) which are not incorporated in the formed ice structure. This increases the salt concentration so that the surrounding unfrozen pore water moves towards the frozen pore in order to dilute the higher salt concentration. In normal pore water of concrete into which no additional salts are introduced there are only few millimoles of dissolved substances and, therefore, the osmotic pressures induced into the concrete matrix do not seem to be large enough to cause the large contraction noticed in concrete during the freezing phase.

In the 1970s, Fagerlund [6] developed the concept of critical degree of saturation in freezing concrete. According to his findings, there is in porous materials a critical degree of saturation which causes deterioration or cracks into the material if the material is frozen even once. The theory was first developed according to the theory of hydraulic pressure but because of the universal nature of the concept it is applicable also to other freezing theories. However, in order to give reasonable results the freezing and thawing cycles by which the

* Tel.: +358 9 451 3770.
E-mail address: vesa.penttala@hut.fi.

0008-8846/$ - see front matter © 2005 Elsevier Ltd. All rights reserved.
doi:10.1016/j.cemconres.2005.10.007

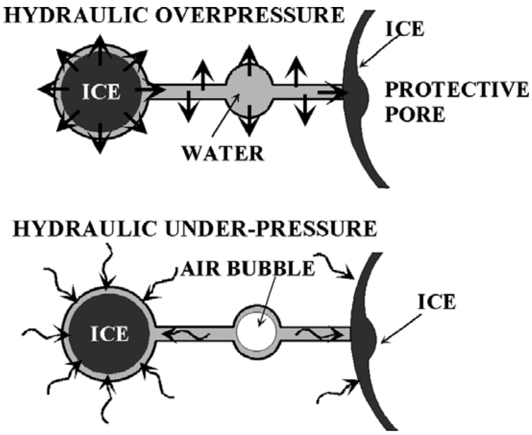

Fig. 1. Water transfer mechanisms in the freezing theories of wet porous materials.

critical degree of saturation is achieved, ought to take place according to the freezing and thawing loads in real structures.

According to Litvan [7–10], water in the capillary pores cannot freeze in situ but the freezing takes place in the vicinity of the outer surface of the structure. The supercooled water causes water movements and drying in the porous body which can cause freezing and thawing deterioration. Setzer [11] took into account the surface forces of the pores and revised Litvan's theory. He was also the first to propose the micro-ice lens theory [12] which explained the water suction from the environment during freezing and thawing cycles. Penttala [13–15] derived a theory based on thermodynamics by which the pressures in pore water can be derived from temperature and relative humidity data measured in concrete during the freezing and thawing cycle. If the amount of pore water is known the pressures in the concrete structures can be calculated. In the theory, the pore size distribution data is not needed. According to the theory based on thermodynamics, the main reason for the pore water movements towards the ice bodies that are first induced is the difference in chemical potential between ice and the unfrozen pore water in the smaller pores surrounding ice and the osmotic pressures play only a minor role.

In the previously mentioned theories (with the exception of the hydraulic pressure theory), the need for air-entrainment, adequate pore size distribution or spacing cannot be calculated. However, the theory of hydraulic pressure is not considered valid in the modeling of freeze–thaw durability of concrete in normal environmental conditions.

There exists a large number of test methods by which the internal damage and surface scaling of concrete can be evaluated. The critical dilation test ASTM C 671 [16] which has now been withdrawn and rapid freezing and thawing test ASTM C 666 [17] are typical tests by which the internal damage of the concrete specimen can be assessed. Salt scaling test ASTM C 672 [18] measures the scaling of the specimen surface in the presence of de-icer salts. There are numerous national freezing and thawing tests that resemble these three which are so-called direct tests performed by using actual freezing and thawing loads. Two recently developed freezing and thawing tests should be mentioned. In the CIF/CDF test [19] and the slab test [20], both internal damage and surface scaling can be determined by the same specimen and test simultaneously. In this research paper, the test results of the latter test method will be presented. Freeze–thaw test results of CIF tests are presented in Refs. [21,22].

2. Frost mechanisms in wet concrete

If the porous material is so wet that the theory of hydraulic over-pressure governs the freezing phenomenon, pore water is squeezed into the larger air-filled pores and the external environment surrounding the sample, and causes there an abrupt increase of relative humidity (Fig. 1). If the pore system is not filled with pore water in the extent that hydraulic pressures are induced into the material (samples are preserved below 97–98% relative humidity) then after the first freezing of the pore water an under-pressure is formed in the pore system and the sample contracts. This is due to pore water transfer towards the newly formed ice lenses because the surface of the ice has a lower chemical potential compared with the chemical potential of the unfrozen pore water surrounding the ice sphere.

In Fig. 2, the strains of a mortar sample having a compressive strength of 40 MPa is studied during a two-cycle freezing and thawing test [23]. The test sample is situated in a low-temperature calorimeter and, thus, the ice amount formed in the sample can be calculated in the test. Even though the mortar sample has been cured under water, no expansion can be detected when the pore water first freezes. After ice has been detected in the mortar sample, a significant contraction can be noticed. Only after the temperature has dropped to around −20 °C, can an expansion be detected. At this temperature, so much ice has been induced into the pore space of the mortar that the newly forming virgin ice cannot expand freely and cracks are formed, and deterioration of mortar commences, which causes residual expansive strains into the specimen.

3. Materials and test arrangements

The surface and internal damages of concrete specimens in non-saline environments during freeze–thaw tests of 45

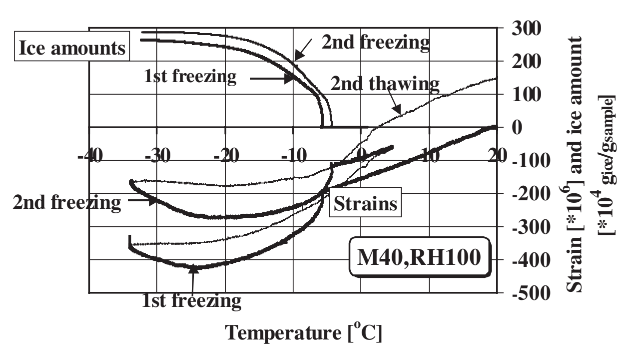

Fig. 2. Strain and ice evolution of a mortar test specimen during a two-cycle freezing and thawing test. Mortar specimen has a compressive strength of 40 MPa and it is cured under water [23].

different concretes were assessed by slab test. The surface and internal damages of salt freeze–thaw tests were studied by 12 different high strength concretes produced in the CONLIFE project [24].

3.1. Freeze–thaw tests

The freeze–thaw tests, in which temperature varied between +20 and −20 °C, were performed with deionized water as the freezing liquid in which no additional salts were dissolved. The test concretes were produced so that a large range of compressive strengths, air contents, curing regimes, and binder amounts were covered. In the tests, surface deterioration was measured by weighing after freezing and thawing. The internal damage in the test slabs was studied by relative dynamic modulus of concrete calculated from the ultrasonic pulse transfer time data of the test slabs.

All test specimens were cast by using the same cement type, CEM IIA 42,5R, of local origin produced by Finnsementti Oy. No other additional binders were used. The petrographic composition of the aggregates was mainly granite and the maximum aggregate diameter was 16 mm except in 8 batches in which it was 8 or 32 mm.

The water–cement ratio of the test concretes was varied so that the test population comprised of concretes having water–cement ratios of 0.30, 0.40, 0.54, 0.65, 0.76, 0.94, and 1.12.

Table 1
Test concrete data of the non-saline freeze–thaw tests

Test concrete	Water/cement ratio	Cement content (kg/m^3)	Water content (kg/m^3)	Aggregate content (kg/m^3)	Maximum aggregate size (mm)	Air content (%)	Curing time (day)	Compressive strength at 28 days (MPa)
1	0.4	475	190	1701	16	1.0	7	61.3
2	0.54	351.9	190	1833	16	0.7	7	55.9
3	0.65	292.3	190	1884	16	0.7	7	44.9
4	0.76	250	190	1921	16	0.6	7	35.8
5	0.94	202.1	190	1962	16	0.7	7	25.3
6	1.12	169.6	190	1990	16	0.9	7	19.8
7	0.4	350	140	1952	16	0.5	7	74.7
8	0.3	450	135	1865	16	0.7	7	79.6
9	0.76	250	190	1921	16	0.6	2	34.3
10	0.76	250	190	1921	16	0.7	4	35.6
11	0.76	250	190	1921	16	0.6	14	36.3
12	0.3	450	135	1865	16	1.1	2	74.3
13	0.3	450	135	1865	16	1.1	4	76.1
14	0.3	450	135	1865	16	1.3	14	81.7
15	0.65	292.3	190	1884	16	0.9	7	47.2
16	0.65	292.3	190	1884	16	1	7	48.1
17	0.65	292.3	190	1884	16	0.8	7	44.4
18	0.65	292.3	190	1884	16	1.4	7	43.0
19	0.76	250	190	1867	16	2.8	7	26.5
20	0.76	250	190	1815	16	4.3	7	28.7
21	0.76	250	190	1842	16	7.5	7	18.8
22	0.76	250	190	1874	16	10.5	7	14.7
23	0.4	475	190	1673	16	3.9	7	58.7
24	0.4	475	190	1610	16	5.9	7	44.4
25	0.4	475	190	1557	16	6.8	7	40.0
26	0.4	475	190	1502	16	9.5	7	34.0
27	0.54	351.9	190	1798	8	0.5	7	56.5
28	0.54	351.9	190	1833	32	1.5	7	52.1
29	0.54	351.9	190	1719	8	4.9	7	42.5
30	0.54	351.9	190	1725	16	5.6	7	36.1
31	0.54	351.9	190	1725	32	5.5	7	36.2
32	0.4	250	100	2142	16	1	7	76.8
33	0.3	351.9	106	2021	16	0.6	7	46.7
34	0.65	351.9	227	1734	16	0.3	7	84.4
35	0.76	351.9	267	1627	16	0.2	7	35.8
36	0.3	450	135	1865	16	0.7	0	71.8
37	0.4	475	190	1720	8	0.8	7	68.6
38	0.4	475	190	1720	32	1.1	7	66.4
39	0.76	250	190	1921	8	0.8	7	33.1
40	0.76	250	190	1921	32	0.5	7	34.9
41	0.4	475	190	1701	16	1	7	67.9
42	0.4	475	190	1701	16	1.4	7	66.6
43	0.76	250	190	1921	16	0.4	7	37.2
44	0.76	250	190	1921	16	1.6	7	31.8
45	0.3	634	190	1560	16	1.4	7	74.0

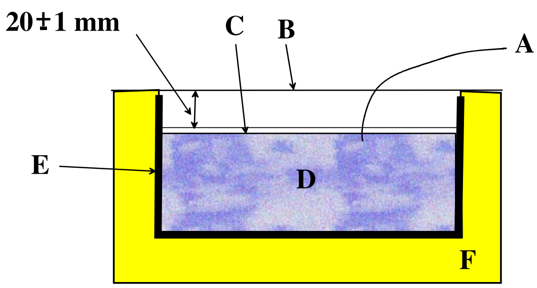

Fig. 3. The test arrangement of the slab test [20]. In the picture A denotes a thermo-element, B is an evaporation protection sheet, C is the freezing liquid, D is the concrete test specimen, E denotes a rubber cover, and F is thermal insulation.

Fig. 4. Surface scaling of 550 g/m^2 of a slab test specimen after 56 freeze–thaw cycles.

The cement content of the test concretes varied from 170 to 634 kg/m^3. The air content of the test concretes varied from 0.6% to 10.5%. The water curing times ranged from 0 to 13 days after the stripping of the moulds at the concrete age of 24 h. Thereafter, the test specimens were stored in a climate cabin at a temperature of 20±2 °C and relative humidity of 65±5%. The amount of the fine aggregates (<0.6 mm) varied from 34 to 384 kg/m^3. The mixture data of the 45 test concretes is presented in Table 1.

The dimensions of the test specimens of the slab test were 150·150·50 mm^3. As an exception to the Swedish standard [20], the freezing surface of the test specimens was the mould surface and not the sawn surface inside the test cube. At the age of 25 days, a rubber sheet was glued on the other faces of the test specimens except the freezing surface of the slab test specimens according to the standard [20] (Figs. 3 and 4). Freezing and thawing tests started at the concrete age of 32 days. The test specimens of the slab tests were weighed for scaling deterioration and the ultrasound measurements were performed after 7, 14, 28, 42, and 56 cycles. The compressive strength of the concretes was measured by loading six 100-mm cubes at the age of 28 days.

3.2. Salt freeze–thaw tests

Salt freeze–thaw tests were performed with 3% NaCl water solution as the freezing liquid. The test concretes were high performance concretes having compressive strength values between 93.3 and 133.9 MPa measured by 100-mm test cubes. In the tests, surface deterioration was measured by weighing the deterioration of the surface layer after freezing and thawing cycles in which temperature varied between +20 and −20 °C. The internal damage in the test slabs was studied by relative dynamic modulus of concrete calculated from the ultrasonic pulse transfer time data of the test slabs.

All these test specimens were cast by using cement type CEM I 52,5 produced by Aalborg Portland AS, Denmark. In 10 of the 12 test concretes condensed silica fume (3% or 10% by cement weight) was used as an additional binder. The aggregates comprised of # 0–2 mm Rhine sand and # 2–16 mm German crushed basalt.

The water–binder ratios of the test concretes were 0.30, 0.35 or 0.42. The cement content of the test concretes varied from 321.9 to 511.2 kg/m^3. The air content of the test concretes varied from 1.7% to 6.5%. The water curing was performed according to the standard [20]. After the first day in the steel moulds, the test samples were stored under water for 6 days. Thereafter, the test specimens were stored in a climate cabin in the temperature of 20±2 °C and relative humidity of 65±5%. The mixture data of the 12 test concretes is presented in Table 2.

Table 2
Test concrete data of the saline freeze–thaw tests

Test concrete	Water/binder ratio	Water/cement ratio	Adjusted water/binder ratio	Aggregate content (kg/m^3)	Cement content (kg/m^3)	Silica fume content (kg/m^3)	Water content (kg/m^3)	Air content (%)	Compressive strength at 28 days (MPa)
46	0.3	0.321	0.273	1960.5	467.3	32.7	112.1	2	128.5
47	0.35	0.375	0.319	2029.1	400.5	28.0	117.6	1.7	127.8
48	0.42	0.449	0.382	2097.7	333.8	23.4	123.0	1.7	110.2
49	0.3	0.305	0.284	1960.7	491.4	14.7	130.5	2	127.4
50	0.3	0.333	0.266	1960.2	450.7	45.1	99.3	2.5	133.9
51	0.42	0.427	0.398	1995.9	351.0	10.5	136.7	5.1	95.3
52	0.42	0.466	0.373	1995.4	321.9	32.2	114.2	5.3	99.9
53	0.3	0.321	0.273	1858.7	467.3	32.7	112.9	6.5	115.8
54	0.35	0.375	0.319	1927.0	400.5	28.0	118.0	4.9	114.8
55	0.42	0.449	0.382	1995.7	333.8	23.4	123.4	4.8	95.2
56	0.3	0.293	0.293	1961.0	511.2	0	145.6	2	127.3
57	0.42	0.411	0.411	1996.1	365.1	0	147.6	5.5	93.9

4. Test results and discussion

4.1. Freeze–thaw tests

The freeze–thaw deterioration test results of the slab tests in which non-saline water was used as freezing liquid are presented in Table 3.

The surface scaling and internal damage test results of the concretes have been analyzed statistically in two parts. Using Statgraphics computer program, most relevant variables were first determined by simple linear regression. Thereafter, the models for these variables were constructed by nonlinear regression.

Table 3
Freeze–thaw deterioration results of the test concretes in which non-saline water was used as freezing liquid

Test concrete	Water/cement ratio	Air content (%)	Curing time (d)	Surface scaling (g/m^2)	Internal damage (RDM %)
1	0.4	1.0	7	25	67
2	0.54	0.7	7	128	52
3	0.65	0.7	7	143	27
4	0.76	0.6	7	1402	0
5	0.94	0.7	7	5129	0
6	1.12	0.9	7	8982.8	0
7	0.4	0.5	7	370	54
8	0.3	0.7	7	91	100
9	0.76	0.6	2	4553	0
10	0.76	0.7	4	3822	0
11	0.76	0.6	14	2532	0
12	0.3	1.1	2	111	100
13	0.3	1.1	4	98	100
14	0.3	1.3	14	23	93
15	0.65	0.9	7	1528	0
16	0.65	1	7	1430	0
17	0.65	0.8	7	2522	0
18	0.65	1.4	7	1378	0
19	0.76	2.8	7	878	74
20	0.76	4.3	7	67	94
21	0.76	7.5	7	59	100
22	0.76	10.5	7	63	100
23	0.4	3.9	7	39	100
24	0.4	5.9	7	19	100
25	0.4	6.8	7	24	100
26	0.4	9.5	7	18	100
27	0.54	0.5	7	2884	16
28	0.54	1.5	7	877	67
29	0.54	4.9	7	18	100
30	0.54	5.6	7	20	100
31	0.54	5.5	7	19	100
32	0.4	1	7	127	100
33	0.3	0.6	7	16	82
34	0.65	0.3	7	2744	1
35	0.76	0.2	7	4088	0
36	0.3	0.7	0	49.1	91
37	0.4	0.8	7	1185	36
38	0.4	1.1	7	941	41
39	0.76	0.8	7	2638	0
40	0.76	0.5	7	3365	1
41	0.4	1	7	41	98
42	0.4	1.4	7	183	49
43	0.76	0.4	7	3976	0
44	0.76	1.6	7	2405	0
45	0.3	1.4	7	54	100

Table 4
The model coefficients of Eq. (1) and the R^2 values of the 45 test concretes in the slab freeze–thaw tests

Damage type	a	b	c	d	e	R^2 (%)
Scaling	−57.80	8679	3.356	0.4957	0.2142	89.2
Internal damage	−831.9	835.0	−0.08153	−0.03092	0.001866	81.1

According to the results obtained from the linear regression calculations, the most relevant variables to model the scaling results were cement content, water content, water–cement ratio, air content, and curing time. In the internal damage modeling, the same variables were the most relevant, with the exception of curing. The best nonlinear regression model of the scaling results was formulated as

$$D = a + b \cdot \lfloor (W/C)^c / A^d / B^e \rfloor \tag{1}$$

in which

- W is water content (kg/m^3),
- C is cement content (kg/m^3)
- A is air content (%)
- B is curing time (day)
- D is deterioration, if surface scaling (g/m^2) or if internal damage relative dynamic modulus RDM in (%), and
- a, b, c, d, e are coefficients.

The most suitable model of the internal damage is

$$D = a + b \cdot \lfloor (W/C)^c / A^d \rfloor. \tag{2}$$

The coefficients of the models and the respective R^2 values are presented in Tables 4 and 5.

The R^2 statistics indicates that the model explains the percentage of the variability in the test in question. The Durbin–Watson [25] statistics of the residuals indicated that there may be some serial correlation in some of the different models. The contours of the estimated response surface of the different tests are presented in Figs. 5–8 by using Eq. (2). An example of the relation of surface scaling and internal damage is presented in Fig. 9.

The R^2 results presented in Tables 4 and 5 show that if the curing measures are included in the model this increases the R^2 values of surface scaling and internal damage slightly. Similarly, as the exponent e of curing time B in Table 4 is a very small number in the internal damage situation, curing measures have very little effect on the internal damage of concrete. This seems quite obvious because curing enhances the quality of the surface layer of concrete, and hence improves the freezing and thawing durability of the surface. Curing increases the hydration degree inside the test slab only

Table 5
The model coefficients of Eq. (2) and the R^2 values of the 45 test concretes in the slab freeze–thaw tests

Damage type	a	b	c	d	R^2 (%)
Scaling	−66.58	5732	3.240	0.4823	87.6
Internal damage	−837.2	836.8	−0.08286	−0.03037	80.8

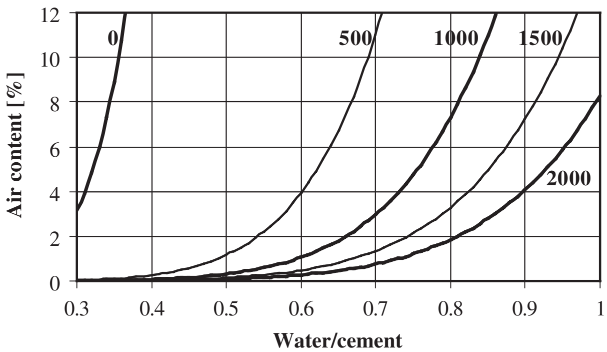

Fig. 5. Contours of the estimated response surface of surface scaling in the slab freeze–thaw tests performed with pure water as the freezing liquid. The numbers beside the curves represent scaling values in (g/m^2).

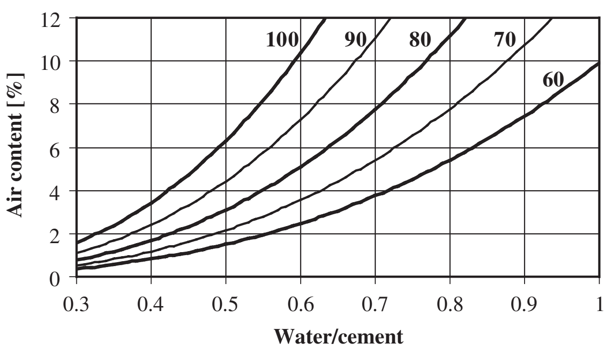

Fig. 6. Contours of the estimated response surface of internal damage in the slab freeze–thaw tests performed with pure water as the freezing liquid. The numbers beside the curves represent internal damage values in relative dynamic modulus (%).

marginally, especially in concretes which are produced by using a low water–cement ratio and, therefore, curing does not effect the internal damage caused by freeze–thaw loads very much.

The R^2 statistics 89.2%, 81.1%, 87.6%, and 80.8% presented in Tables 4 and 5 can be considered quite high taking into consideration the large variability in the composition of the test concretes. The two freeze–thaw deterioration values D can be modeled with quite high statistical relevancy using only two variables, water–cement ratio and air content,

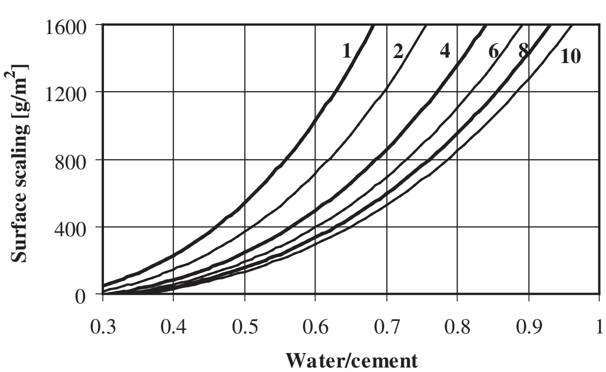

Fig. 7. Contours of the estimated response surface of surface scaling in the slab freeze–thaw tests using non-saline water as the freezing liquid. The numbers beside the curves represent air content values in (%).

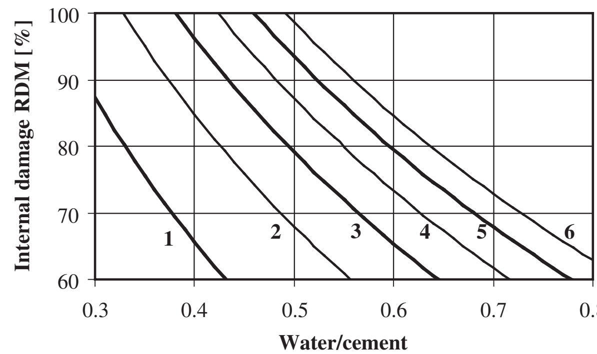

Fig. 8. Contours of the estimated response surface of internal damage in the slab freeze–thaw tests using non-saline water as the freezing liquid. The numbers beside the curves represent air content values in (%).

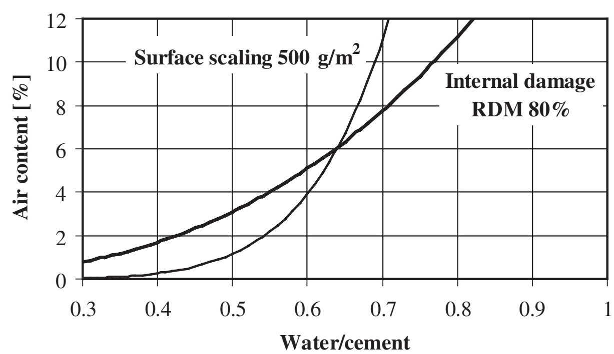

Fig. 9. Two contours of the estimated response surfaces of surface scaling and internal damage results in the slab freeze–thaw tests in which pure water was used as the freezing liquid.

even though water–cement ratio varies from 0.3 to 1.12 and air content varies from 0.6% to 10.5%. However, it should be taken into consideration that only one cement type and aggregate type is used.

In Fig. 9, it can be seen that during an increase in the water–cement ratio of concrete, the need for air-entrainment increases as surface scaling damage evolves much faster compared to the internal damage failure mode. On the other hand, in concretes possessing low water–cement ratios the most important criterion for the air content comes from the internal damage curve in this figure.

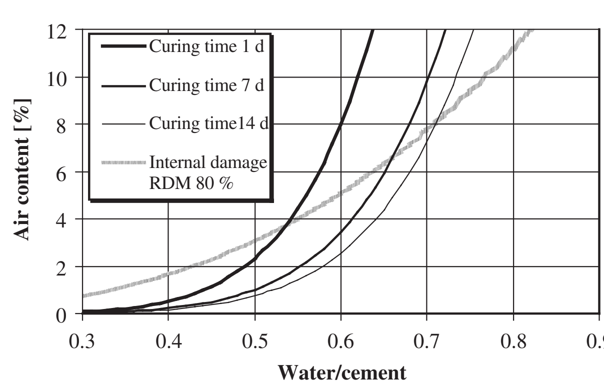

Fig. 10. Comparison of the effect of water curing on the surface scaling of 200 g/m^2 in the slab test by using Eq. (1).

Table 6
Freeze–thaw deterioration results of the test concretes in which saline water was used as freezing liquid

Test concrete	Water/binder ratio	Water/cement ratio	Air content (%)	Compressive strength at 28 days (MPa)	Surface scaling (g/m^2)	Internal damage (RDM %)
46	0.3	0.321	2	128.5	138	35
47	0.35	0.375	1.7	127.8	520	17
48	0.42	0.449	1.7	110.2	1568	17
49	0.3	0.305	2	127.4	56	58
50	0.3	0.333	2.5	133.9	54	58
51	0.42	0.427	5.1	95.3	61	97
52	0.42	0.466	5.3	99.9	137	92
53	0.3	0.321	6.5	115.8	118	101
54	0.35	0.375	4.9	114.8	100	99
55	0.42	0.449	4.8	95.2	255	43
56	0.3	0.293	2	127.3	67	59
57	0.42	0.411	5.5	93.9	54	92

Table 7
The model coefficients of Eq. (2) and the R^2 values of the 12 test concretes in the slab salt freeze–thaw tests

Damage type	a	b	c	d	R^2 (%)
Scaling	24.91	1111300	6.698	2.294	98.6
Internal damage	234.6	−360.7	0.3683	0.3388	81.7

One of the biggest merits of the slab and CIF tests is that both the surface scaling and the internal damage can be assessed from the same test specimen in a single test so that the two deterioration mechanisms do not interfere with each others test result in the same extent as in other freezing and thawing tests. Similarly, the thermodynamic pumping effect is taken into consideration in these tests and the freezing action is taking place only in one direction. The test results give a good basis in estimating the service life prediction of concrete structures.

The effect of water curing is compared in Fig. 10. The curing time has a remarkable effect on the air content requirement at the water–cement ratio in question. In the internal damage situation, the effect of curing is negligible.

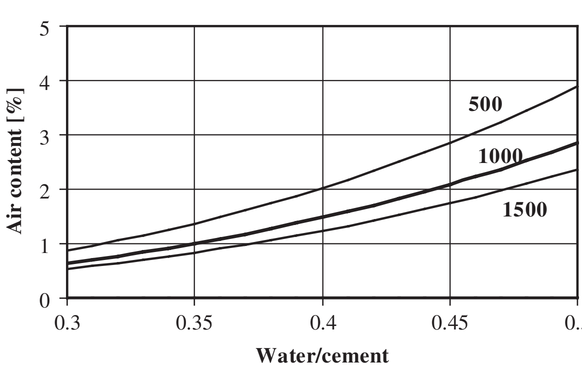

Fig. 11. Contours of the estimated response surface of surface scaling in the slab freeze–thaw tests performed with saline water as the freezing liquid. The numbers beside the curves represent scaling values in (g/m^2).

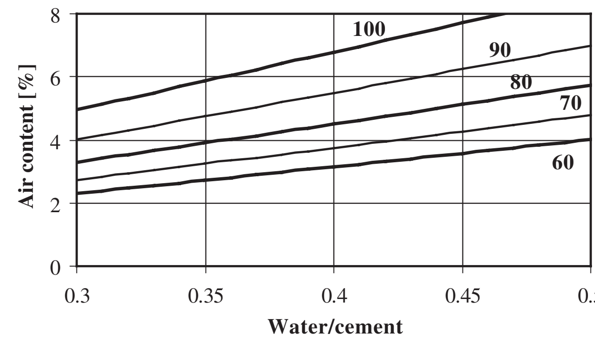

Fig. 12. Contours of the estimated response surface of internal damage in the slab freeze–thaw tests performed with saline water as the freezing liquid. The numbers beside the curves represent internal damage values in relative dynamic modulus (%).

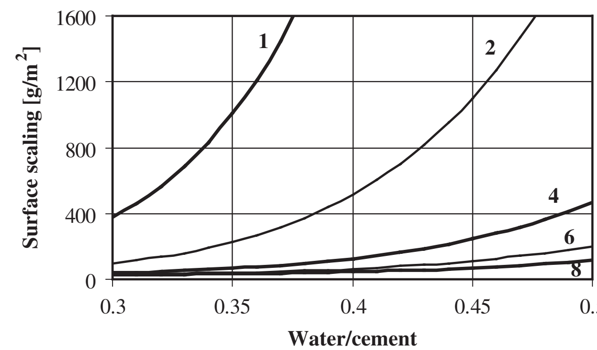

Fig. 13. Contours of the estimated response surface of surface scaling in the slab freeze–thaw tests using saline water as the freezing liquid. The numbers beside the curves represent air content values in (%).

4.2. Salt freeze–thaw tests

The freeze–thaw deterioration test results of the slab tests in which saline water was used as freezing liquid are presented in Table 6.

Because curing time was not varied, deterioration Eq. (2) is used for both surface scaling and internal damage. The coefficients of the models and the respective R^2 values are presented in Table 7.

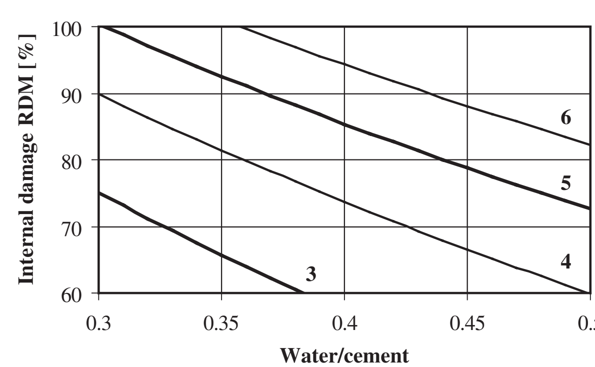

Fig. 14. Contours of the estimated response surface of internal damage in the slab freeze–thaw tests using saline water as the freezing liquid. The numbers beside the curves represent air content values in (%).

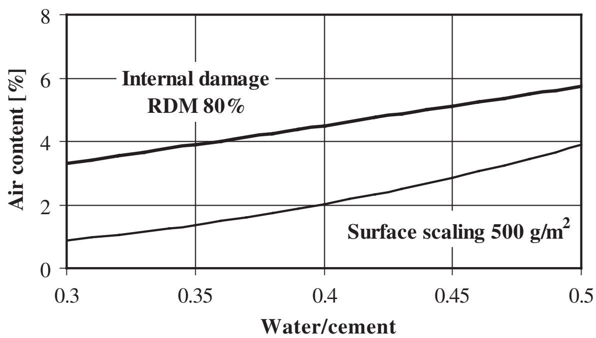

Fig. 15. Two contours of the estimated response surfaces of surface scaling and the internal damage results in the slab freeze–thaw tests in which saline water was used as the freezing liquid.

The R^2 statistics of surface scaling model of the salt freeze–thaw test specimens is extremely high 98.6% while the internal damage value 81.7% is of the same order of magnitude as in the models construed by freeze–thaw test results done by non-saline freezing liquid.

The contours of the estimated response surface of the different deterioration mechanisms are presented in Figs. 11–14 using Eq. (2). An example of the relation of surface scaling and internal damage is presented in Fig. 15.

In Fig. 15, it can be noticed that in high strength concretes the internal damage in the salt freeze–thaw test is the major deterioration mechanism when water–cement ratio is below 0.5. If concretes had been produced with a higher water–cement ratio, the scaling curve would have crossed the internal damage curve at higher water–cement ratio values similar to the non-saline freeze–thaw situation.

5. Conclusions

Surface scaling and internal damage freeze–thaw deterioration was modeled by using test results of 45 concretes frozen in a non-saline environment and by using test results of 12 high-strength concretes when saline freezing liquid was used. Statistically, the most important variables were water–cement ratio, air content, and curing time. Curing time improved the surface scaling deterioration values in the non-saline freeze–thaw tests, but curing had only a very small effect on the internal damage in the tests. The R^2 values of the models ranged from 80.8% to 89.2% with the exception of surface scaling model in saline freeze–thaw test in which it was 98.6%.

The test results showed that internal damage determines the need for air-entrainment in high-strength concretes while in normal or low-strength concretes, surface scaling determines the need for higher air content compared to the internal damage freeze–thaw mechanism.

One of the biggest merits of the slab and CIF/CDF tests is that both the surface scaling and the internal damage can be assessed from the same test specimen in a single test so that the two deterioration mechanisms do not interfere with each others test result in the same extent as in the other contemporary freezing and thawing tests. Similarly, the thermodynamic pumping effect is taken into consideration in these tests and the freezing action is taking place only in one direction.

References

[1] T.C. Powers, Journal of the American Concrete Society 16 (1945) 245.
[2] T.C. Powers, Proceedings of the Highway Research Board, Portland Cement Association, Bulletin, vol. 33, 1949, p. 1.
[3] T.C. Powers, T.L. Brownyard, Journal of the American Concrete Institute 18 (1947) 549.
[4] T.C. Powers, T.L. Brownyard, Journal of the American Concrete Institute 18 (1947) 933.
[5] T.C. Powers, R.A. Helmuth, Proceedings of the Highway Research Board, vol. 32, 1953, p. 285.
[6] G. Fagerlund, Materials and Structures 58 (1977) 217.
[7] C.G. Litvan, Journal of Colloid and Interface Science 38 (1972) 75.
[8] E.W. Sidebottom, C.G. Litvan, Transactions of the Faraday Society 585, 67 (1971) 2726.
[9] C.G. Litvan, Journal of the American Ceramic Society 55 (1971) 38.
[10] C.G. Litvan, Journal of Colloid and Interface Science 45 (1973) 154.
[11] M.J. Setzer, Deutscher Ausschuss für Stahlbeton Heft 280 (1977) 43.
[12] M.J. Setzer, Proceedings of the International RILEM Workshop on Resistance of Concrete to Freezing and Thawing with or without De-icing Chemicals, Proceedings, vol. 34, 1997, p. 157.
[13] V. Penttala, Advanced Cement Based Materials 7 (1998) 8.
[14] V. Penttala, Concrete Science and Engineering 1 (1999) 2.
[15] V. Penttala, F. Al-Neshawy, Cement and Concrete Research 32 (2002) 1407.
[16] ASTM Standard C 671-86, Standard Test Method for Critical Dilation of Concrete Specimens Subjected to Freezing, American Society for Testing and Materials, Philadelphia, 1991.
[17] ASTM Standard C 666-90, Standard Test Method for Resistance of Concrete to Rapid Freezing and Thawing, American Society for Testing and Materials, Philadelphia, 1991.
[18] ASTM Standard C 672-91, Standard Test Method Scaling Resistance of Concrete Surfaces Exposed to Deicing Chemicals, American Society for Testing and Materials, Philadelphia, 1991.
[19] Recommendations of RILEM TC 176-IDC: test methods of frost resistance of concrete. CIF-test-capillary suction, internal damage and freeze thaw test, reference method and alternative methods A and B, Materials and Structures, vol. 34, 2001, p. 515.
[20] Swedish standard SS13 72 44:1988, Betongprovning-hårdnad betong-frost. Stockholm (1988).
[21] V. Penttala, V. Räsänen, 11th International Congress on the Chemistry of Cement, ICCC 2003. Durban, South-Africa, 11–16 May, 2003, p. 1535.
[22] V. Penttala, F. Al-Neshawy, T. Lehtinen, V. Räsänen, Internal and surface deterioration of concrete due to frost action: 15. Internationale Baustofftagung IBAUSIL, 24.–27.9.2003, Band 2. Weimar, Germany, 2003, p. 0601.
[23] V. Penttala, F. Al-Neshawy, Frost Damage in Concrete, Minneapolis, USA, 28–30 June. France, Rilem Publications Sarl, RILEM Proceedings PRO, vol. 25, 1999, p. 115.
[24] V. Penttala, A. Cwirzen, Proceedings of international conference on durability of HPC and final workshop of CONLIFE, University of Duisburg-Essen, IBPM, 23–24 September, 2004, Essen, Germany, 2004, p. 197–206.
[25] N. Draper, H. Smith, Applied Regression Analysis, Wiley, New York, 1981, 699 pp.